Quantum-mechanical model of Fermi-surface traversal resonance

A. Ardavan, S. J. Blundell, and J. Singleton
University of Oxford, Department of Physics, Clarendon Laboratory, Oxford OX1 3PU, United Kingdom
(Received 7 July 1999)

We describe a quantum-mechanical model of Fermi-surface traversal resonance (FTR), a magneto-optical resonance that occurs in quasi-one-dimensional metals. We show that the predictions of this model are in quantitative agreement with earlier semiclassical models of FTR. The agreement between the two approaches, whose starting assumptions are very different, demonstrates that it is a fundamental property of quasi-one-dimensional systems. [S0163-1829(99)03047-7]

Recently, efforts have been made to measure high-frequency effects, such as cyclotron resonance (CR), in low-dimensional metals, motivated initially by the predictions that comparisons of the dynamical mass (measured in CR experiments) with the ''bare'' band mass (from band-structure calculations) and the effective mass (from analysis of the temperature dependence of quantum oscillations), should yield information about the nature of the inter-carrier interactions in these materials.[1,2] This work led to the prediction[3] and observation[4] of Fermi-surface traversal resonance (FTR), an analogue of CR, which arises from the open orbits across quasi-one-dimensional (Q1D) Fermi-surface (FS) sections. Until now, all theoretical models of FTR (including recent work on weakly incoherent models[5]) have been derived in the semiclassical limit, $\hbar \rightarrow 0$. In this paper we present a simple quantum-mechanical model that quantitatively reproduces the properties of FTR's predicted by the semiclassical models.

We begin by briefly summarizing the semiclassical model and its results. More detailed descriptions can be found in Refs. 4 and 6. The real-space structure of a quasi-one-dimensional metal is characterized by the presence of chains along which carriers can move freely and between which they can hop with a probability proportional to the nearest-neighbor transfer integral t. The momentum-space structure is characterized by a Fermi surface comprised of weakly warped planes. The real-space velocity of a carrier (which is in the direction perpendicular to the Fermi surface)[3,4,7] lies predominantly in one direction (the chain direction) but can also have components, v_t, proportional to t perpendicular to the chain direction.

When a magnetic field B is applied perpendicular to both the chain direction and the interchain transfer direction, a carrier experiences the Lorentz force and sweeps across the Fermi sheet in the direction of the warping. The component of its real-space velocity parallel to the sheet oscillates at a frequency $\omega_{1D}=eBbv_F/\hbar$, where e is the carrier's charge, b is the chain separation in real space, and v_F is the Fermi velocity.[4,6] The carrier can thus absorb energy from an electric field that is polarized parallel to the oscillatory component of the velocity and is oscillating at the frequency ω_{1D}. This effect is exhibited as a resonance, FTR, in the high-frequency conductivity $\sigma(\omega)$; the amplitude of the resonance in $\sigma(\omega)$ is proportional to v_t^2. The intensity of the magneto-optical absorption is proportional to $\sigma(\omega)^2$, and scales as t^4. Higher-order transfer integrals cause harmonics in the warping of the Fermi sheet and, hence, harmonics in the oscillating velocity and harmonics of FTR; the frequency of the nth harmonic is $n\omega_{1D}$.

Our quantum-mechanical model is an extension of the method of Yakovenko and Goan[8] and is mathematically similar to the description of the Wannier-Stark ladder.[9] Consider a set of chains, each parallel to x, labeled by the index n and separated by a distance b in the y direction; carriers move freely along the chains. In the absence of any interactions between the chains, the eigenfunctions of the system are given by the product of a plane wave along the chain and a transverse wave function representing the occupation of a particular chain, $|\psi\rangle=e^{ik_x x}|\phi_n\rangle$. We use the linearized Hamiltonian, $\mathcal{H}=\hbar v_F \hat{k}_x$, since we consider only the carriers close to the Fermi surface. Since the carriers are confined to a single chain, the only contribution to the energy is from motion along the chain, and the corresponding Fermi surface is formed by the planes $k_x=\pm k_F$.

Adding hopping between the chains, the Hamiltonian becomes

$$\mathcal{H}=\hbar v_F \hat{k}_x - \sum_{i,n} t_i (c_{n+i}^{\dagger} c_n + c_{n-i}^{\dagger} c_n), \tag{1}$$

where $c_{n+i}^{\dagger} c_n |\phi_n\rangle = |\phi_{n+i}\rangle$ and t_i gives the strength of the transfer between chains i apart. The presence of a hopping term allows carriers to move in the transverse direction, implying that the corresponding Fermi surface is warped. Indeed, the t_i in Eq. (1) are closely related to the transfer integrals used in tight-binding calculations of the band structure[10] and the t used in the semiclassical theory of FTR. Since a carrier is no longer confined to a particular chain, its wave function is now distributed across many chains; the eigenstates become

$$e^{ik_x x}|\xi_m\rangle = e^{ik_x x}\sum_n a_{mn}|\phi_n\rangle. \tag{2}$$

We apply a magnetic field, choosing a gauge such that the vector potential is $\mathbf{A}=(-By,0,0)$, by applying the transformation $\hbar\hat{k}_x \rightarrow \hbar\hat{k}_x + qA_x = \hbar\hat{k}_x - qBy = \hbar\hat{k}_x + eBnb$. Thus, the Hamiltonian becomes

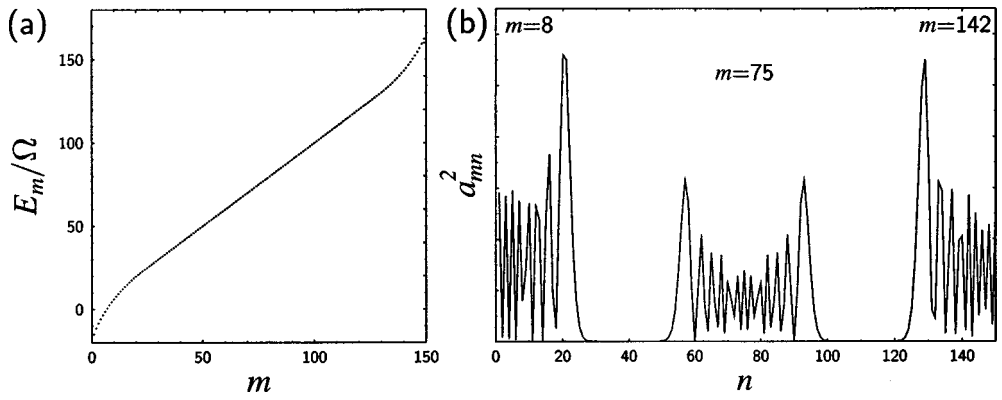

FIG. 1. Results of the diagonalization of $\mathcal{H}$ for $t_1=10\Omega$. (a) The eigenenergies, E_m of $|\xi_m\rangle$. (b) The probability density functions of states $|\xi_8\rangle$, $|\xi_{75}\rangle$, and $|\xi_{142}\rangle$. These are given by $|a_{mn}|^2=a_{mn}{}^2$ (because a_{mn} are real).

$$\mathcal{H}=v_F\left(-i\hbar\frac{\partial}{\partial x}+eBnb\right)-\sum_{i,n}t_i(c_{n+i}^{\dagger}c_n+c_{n-i}^{\dagger}c_n). \quad (3)$$

Operating on the set of transverse basis states $|\phi_n\rangle$ with $\mathcal{H}$, we find that

$$\mathcal{H}|\phi_n\rangle=n\Omega|\phi_n\rangle-\sum_i t_i(|\phi_{n+i}\rangle+|\phi_{n-i}\rangle), \quad (4)$$

where $\Omega=eBbv_F$. If we confine the carriers to only the chains $1<n<N$, by imposing the boundary conditions $|\phi_n\rangle=0$ for $n<1$ and $n>N$, the Hamiltonian can be written as a finite matrix,

$$\mathcal{H}=\begin{pmatrix}\Omega & -t_1 & -t_2 & -t_3 & \cdots & -t_{N-1} & -t_N\\ -t_1 & 2\Omega & -t_1 & -t_2 & \cdots & -t_{N-2} & -t_{N-1}\\ -t_2 & -t_1 & 3\Omega & -t_1 & \cdots & \cdots & \cdots\\ \vdots & \vdots & \ddots & \ddots & \ddots & \vdots & \vdots\\ -t_{N-1} & -t_{N-2} & \cdots & \cdots & \cdots & (n_N-1)\Omega & -t_1\\ -t_N & -t_{N-1} & \cdots & \cdots & \cdots & -t_1 & n_N\Omega\end{pmatrix} \quad (5)$$

that can be diagonalized numerically. The components of the mth eigenvector of this matrix are the a_{mn} in Eq. (2), and the eigenvalues are the corresponding transverse-motion energy levels of the system.

We first consider the case for which there are no interchain interactions, $t_i=0$ for all i. The matrix in Eq. (5) is already diagonal, and the states $|\phi_n\rangle$ are the transverse eigenstates. Operating on the full eigenstates of the system, $|\psi\rangle=e^{ik_xx}|\phi_n\rangle$, with $\mathcal{H}$, we find that the eigenenergies are

$$E_n=\hbar v_Fk_x+n\Omega. \quad (6)$$

The first term corresponds to the energy associated with the momentum along the chain. The second term is a ladder of energies associated with the transverse motion; the energy separation of the states in this ladder, Ω, matches the energy of the FTR resonance obtained semiclassically, $\omega_{1D}/\hbar$. Semiclassically, FTR is excited by an oscillatory electric field polarized along y; here, the transition strength is given by

$$\left|\int\langle\phi_n|e^{-ik_xx}\hat{y}e^{ik_x'x}|\phi_m\rangle dx\right|^2 = \left|\langle\phi_n|\hat{y}|\phi_m\rangle\int e^{i(k_x'-k_x)x}dx\right|^2, \quad (7)$$

where the integral is over the length of the chain. Thus the transition strength is zero for $k_x\neq k_x'$, and the dipole transition conserves the intrachain momentum. The change of energy is therefore simply $(n-m)\Omega$. This is generally true, and in the discussion that follows, we shall consider only the transverse part of the wave functions.

In fact, the matrix element $\langle\phi_n|\hat{y}|\phi_m\rangle$ is zero and so when $t_i=0$, optical transitions between the eigenstates are not possible. This is to be expected; semiclassically, this corresponds to the case where the Fermi sheet is not warped and the carrier's real-space velocity does not oscillate as it crosses the sheet. Thus, it cannot cause a resonance in the high-frequency conductivity by coupling to an oscillatory electric field.

Sinusoidal warping of the Fermi sheet is introduced by making t_1 nonzero. Figure 1(a) shows the eigenenergies of

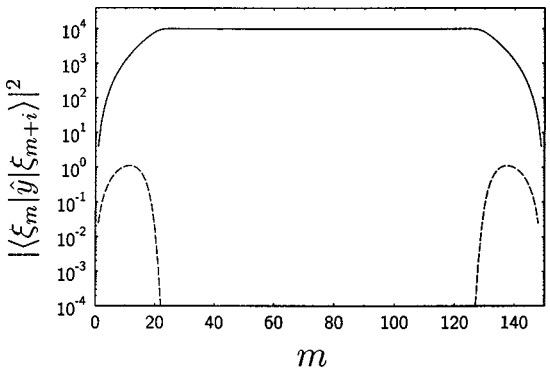

FIG. 2. Transition matrix elements $|\langle\xi_m|\hat{y}|\xi_{m+i}\rangle|^2$ for $i=1$ (solid) and $i=2$ (dashed), calculated for $t_1=10\Omega$.

the new eigenstates $|\xi_m\rangle$, E_m/Ω, plotted against m, obtained by diagonalizing $\mathcal{H}$ for the case where $t_1=10\Omega$, $N=150$, and $e=B=b=1$. Again, the eigenenergies form a ladder $E_m=m\Omega$, except near the edges; the significance of the states near the edges is discussed below. Figure 1(b) shows $|a_{mn}|^2$ plotted against n for the three eigenstates $m=8$, 75, and 142. $|a_{mn}|^2$ is the probability that, in the mth eigenstate, the nth chain is occupied. The plots in Fig. 1(b) can therefore be thought of as real-space probability density functions for the eigenstates $|\xi_8\rangle$, $|\xi_{75}\rangle$, and $|\xi_{142}\rangle$.

$|\xi_{75}\rangle$ is a state that exists entirely within the bulk of the material; the probability density is localized within a band well away from the edges of the crystal (i.e., well away from the chains $n=1$ and $n=150$). Within the band, the probability density is concentrated toward the edges. Semiclassically, the particle is moving along the chain direction with a sinusoidal transverse oscillation. It spends longer near the limits of its excursion than near the center, since the transverse velocity is smallest at the limits of the transverse motion. The states $|\xi_8\rangle$ and $|\xi_{142}\rangle$ are edge states; their probability density functions do not vanish at the edges. The corresponding semiclassical orbits are skipping orbits, with the particle executing sinusoidal motion between successive reflections from the crystal edge. The difference between the edge states and bulk states is also reflected in their eigenenergies. The energies of the bulk states still form a ladder of energies separated by Ω, but the energies of the edge states are modified by the extra confinement caused by the proximity of the crystal edge, and the separation of energies increases. This is the reason for the deviation of the energies plotted in Fig. 1(a) from a straight line toward the crystal edges.

With interchain hopping in place, dipole transitions are possible between the states $|\xi_m\rangle$. Figure 2 shows the first-order dipole transition matrix elements $|\langle\xi_m|\hat{y}|\xi_{m+1}\rangle|^2$ plotted on a logarithmic scale against m (solid line). The second-order matrix elements $|\langle\xi_m|\hat{y}|\xi_{m+2}\rangle|^2$ are also plotted (dashed line). The first-order transition matrix elements between neighboring bulk states are uniform, with an energy Ω. These transitions correspond to the first harmonic of FTR's in the semiclassical model.

Second-order transitions are not allowed between the bulk states. This is also consistent with the semiclassical description; harmonics of FTR occur when the real-space velocity of the carrier contains harmonics. It is interesting to note, however, that second- and higher-order transitions do occur between edge states; this is because, even in the absence of higher-order t_i, the real-space velocity of the edge states, whose orbits are skipping orbits, have higher harmonic content as a result of the skipping. Such skipping orbits have been encountered before; the effects of magnetic-field-induced skipping orbits at the surface of conventional metals were studied experimentally in the 1960s by Koch and Kuo[11] and interpreted in terms of a quantum-mechanical model,[12] and in the 1980s, Merkt measured and modeled the band structure and optical properties of carriers at the surface of InSb (a semiconductor) in crossed electric and magnetic fields, including the effects of skipping orbits.[13]

If the ratio Ω/t_1 is increased (i.e., the magnetic-field strength is increased for a constant hopping interaction), it is found that the probability density functions of the states $|\xi_m\rangle$ become narrower; the effect of the magnetic field is to confine the carriers to narrower orbits. This effect is also observed in the semiclassical model. This one dimensionalization and its consequent effects have been discussed by Dupius and Montambaux.[14] At large magnetic fields, the carrier is confined to a very few chains; the model presented here breaks down in this limit, where the approximation of a discretized wave function is no longer valid (in this model, the wave function is only defined on the chains, at $y=nb$). The validity of the semiclassical model also becomes doubtful in this limit; it is inappropriate to consider the magnetic-field-induced confinement of a carrier to just a few unit cells in the semiclassical limit.

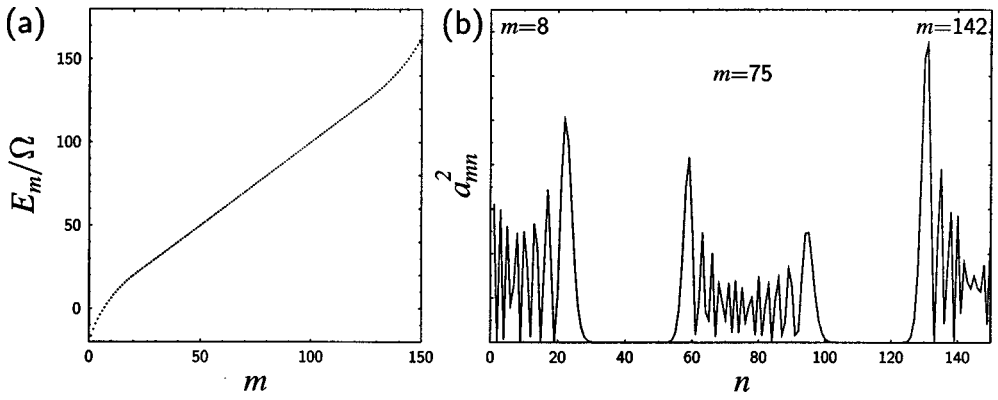

FIG. 3. Results of the diagonalization of $\mathcal{H}$ for $t_1=10\Omega$ and $t_2=t_1/10$. (a) The eigenenergies, E_m of $|\xi_m\rangle$. (b) The probability density functions of states $|\xi_8\rangle$, $|\xi_{75}\rangle$, and $|\xi_{142}\rangle$.

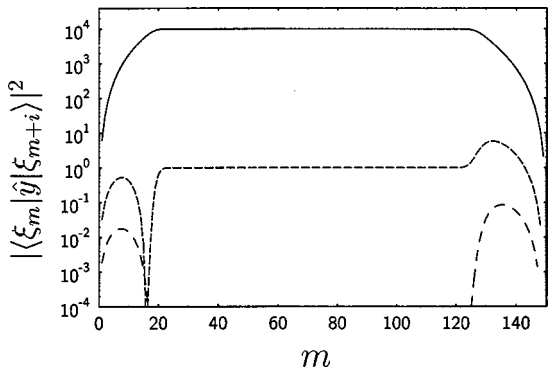

FIG. 4. Transition matrix elements $|\langle\xi_m|\hat{y}|\xi_{m+i}\rangle|^2$ for $i=1$ (solid), $i=2$ (dashed), and $i=3$ (dotted) calculated for $t_1=10\Omega$, $t_2=t_1/10$.

The correspondence with the semiclassical description continues when higher-order transfer integrals are included. Figure 3 shows the eigenenergies and eigenstates obtained by diagonalizing $\mathcal{H}$ with $t_1=10\Omega$, $t_2=t_1/10$, and $N=150$. As before, the energies of the bulk states form a ladder with a separation Ω, with deviations from the ladder by the edge states. The most notable difference between the bulk states shown in Figs. 3(b) and 1(b) is that the probability density function, while still peaked at the limits, is no longer symmetrical about the central occupied chain. In the semiclassical model, the real-space velocity of the orbit now contains a second-harmonic component; thus, the real-space orbit path becomes somewhat sawtooth shaped, and the carrier spends more time to one side of the orbit. This is reflected in the asymmetry of the quantum-mechanical probability density function. The asymmetry of the probability density function depends on the sign of t_2; reversing the sign of t_2 mirrors the probability density function about the central occupied chain.

The presence of the second harmonic in the real-space velocity gives rise to a second harmonic of the FTR in the semiclassical model. Correspondingly, the second-order transition matrix element $|\langle\xi_m|\hat{y}|\xi_{m+2}\rangle|^2$, shown dashed in Fig. 4, is now finite for bulk states. These transitions are between states with an energy difference of 2Ω. Since Ω is proportional to the magnetic-field strength, in a swept-field experiment these second-order transitions will occur at a magnetic field that is half as strong as the field for the fundamental resonance; they correspond to the second harmonic of FTR in the semiclassical model, occurring at a frequency of $2\omega_{1D}$. For this case, where $t_2/t_1=10^{-1}$, the ratio of the second-order transition matrix elements to first-order transition matrix elements is 10^{-4}. Figure 4 also shows the third-order transition matrix elements $|\langle\xi_m|\hat{y}|\xi_{m+3}\rangle|^2$, which are zero for the bulk states, since t_3 is zero (though third-order transitions occur between edge states for the reasons given above). In general, we find that if t_i is nonzero, then ith-order transitions are allowed between bulk states, and the transition intensity scale as by t_i^4, in agreement with the predictions of the semiclassical model.

The significance of the agreement between the two models lies in the fact that they each predict the effect from quite different initial assumptions. In the semiclassical limit, the granularity of the lattice is reflected only in the existence of the Brillouin zone and the Fermi surface; particles are considered to be pointlike in both real space and momentum space and are allowed to move continuously. In the quantum-mechanical model, the granularity of the lattice appears explicitly; we consider the occupancy of each chain individually. The prediction of FTR by both models indicates that it is a fundamental property of quasi-one-dimensional systems.

The authors would like to thank V. Yakovenko, F. Peeters, and J. Chalker for very helpful discussions. This work was supported by the EPSRC.

[1] J. Singleton *et al.*, Phys. Rev. Lett. **68**, 2500 (1992); S. Hill *et al.*, Synth. Met. **55-57**, 2566 (1993); **70**, 821 (1995); A. Polisski *et al.*, J. Phys.: Condens. Matter **8**, L195 (1996); S. V. Demishev *et al.*, Phys. Rev. B **53**, 12 794 (1996); A. Ardavan *et al.*, Synth. Met. **85**, 1501 (1997); H. Ohta *et al.*, *ibid.* **86**, 2011 (1997); **86**, 1913 (1997); A. Polisski *et al.*, *ibid.* **86**, 2197 (1997); S. Hill *et al.*, Physica B **246-247**, 110 (1998).

[2] S. Hill, J. S. Brooks, Z. Q. Mao, and Y. Maeno, cond-mat/9905147 (unpublished).

[3] S. J. Blundell, A. Ardavan, and J. Singleton, Phys. Rev. B **55**, 6129 (1997).

[4] A. Ardavan, J. M. Schrama, S. J. Blundell, J. Singleton, W. Hayes, M. Kurmoo, P. Day, and P. Goy, Phys. Rev. Lett. **81**, 713 (1998).

[5] R. McKenzie and P. Moses, Phys. Rev. B **60**, 11 241 (1999).

[6] A. Ardavan, J. M. Schrama, S. J. Blundell, J. Singleton, A. Semeno, P. Goy, M. Kurmoo, and P. Day, Proc. SPIE **3828**, 366 (1999).

[7] S. J. Blundell and J. Singleton, Phys. Rev. B **53**, 5609 (1996).

[8] V. M. Yakovenko and H.-S. Goan, Phys. Rev. B **58**, 8002 (1998).

[9] G. H. Wannier, Phys. Rev. **117**, 432 (1960).

[10] T. Ishiguro, K. Yamaji, and G. Saito, *Organic Superconductors* (Springer-Verlag, Berlin, 1996), Chap. 3.

[11] J. F. Koch and C. C. Kuo, Phys. Rev. **143**, 470 (1966).

[12] J. F. Koch, University of Maryland, Technical Report No. 744 (unpublished).

[13] U. Merkt, Phys. Rev. B **32**, 6699 (1985).

[14] N. Dupuis and G. Montambaux, Phys. Rev. Lett. **68**, 357 (1992); Phys. Rev. B **46**, 9603 (1992).